



Bi₃In₄S₁₀ and Bi_{14.7}In_{11.3}S₃₈: Two new bismuth sulfides with interesting Bi–Bi bonding

Wenlong Yin^{a,b,c}, Dajiang Mei^{a,b,c}, Jiyong Yao^{a,b,*}, Peizhen Fu^{a,b}, Yicheng Wu^{a,b}

^a Center for Crystal Research and Development, Technical Institute of Physics and Chemistry, Chinese Academy of Sciences, Beijing 100190, P.R. China

^b Key Laboratory of Functional Crystals and Laser Technology, Chinese Academy of Sciences, Beijing 100190, P.R. China

^c Graduate University of Chinese Academy of Sciences, Beijing 100049, P.R. China

ARTICLE INFO

Article history:

Received 7 June 2010

Received in revised form

13 August 2010

Accepted 22 August 2010

Available online 27 August 2010

Keywords:

Bismuth

Indium

Sulfide

Crystal structure

Optical

ABSTRACT

Two new ternary bismuth chalcogenides, Bi₃In₄S₁₀ and Bi_{14.7}In_{11.3}S₃₈, were synthesized from the reactions of binary sulfides via a two-step flux technique. Single-crystal X-ray diffraction analyses indicate that Bi₃In₄S₁₀ crystallizes in the non-centrosymmetric space group *Pm* and Bi_{14.7}In_{11.3}S₃₈ crystallizes in the centrosymmetric space group *P2₁/m*. Both compounds adopt three-dimensional frameworks. A distinct structural feature in the two structures is the presence of chains of Bi atoms with alternating short Bi–Bi bonds of around 3.1 Å and longer distances of around 4.6 Å. The optical band gaps of 1.42(2) eV for Bi₃In₄S₁₀ and 1.45(2) eV for Bi_{14.7}In_{11.3}S₃₈ were deduced from the diffuse reflectance spectra.

© 2010 Elsevier Inc. All rights reserved.

1. Introduction

Bismuth chalcogenides are an interesting class of materials because they not only possess amazing structural and compositional complexity [1] but also have potential applications as nonlinear optical materials [2–4], photoelectrics [5], and thermoelectrics [6–9]. The stereochemical activity of 6s² lone pair of electrons of Bi affects both the structure and the properties of the resulting compounds [4,7,8]. For this reason the exploratory synthesis of new bismuth chalcogenides has been an active area for decades and many bismuth chalcogenides with interesting structures and properties have been discovered [4,7–14]. For example, CsBi₄Te₆ [7] and K₂Bi₈Se₁₃ [8] possess attractive thermoelectric properties and Cs₅BiP₄Se₁₂ exhibits very large second harmonic generation effect [4]. On the other hand, Indium chalcogenides are another class of materials with important properties. For example LiInQ₂ (Q=S, Se) are excellent IR nonlinear optical materials [15], while CuInQ₂ are important solar cell materials [16]. Clearly, the macroscopic physical properties of these compounds stem from both the bonding nature of microscopic building blocks, i.e. the Bi–Q or In–Q polyhedra, and the packing of these building blocks in the structure. Thus the combination of bismuth and indium in one chalcogenide may generate compounds with interesting structures and properties through the interplay of the Bi–Q and In–Q polyhedral building blocks.

* Corresponding author. Fax: +86 10 82543725.
E-mail address: jyao@mail.ipc.ac.cn (J. Yao).

In the Bi/In/Q (Q=S, Se, Te) system, only four sulfides were reported, namely BiInS₃, Bi₂In₄S₉, Bi₄In₂S₉, and Bi₃In₅S₁₂ [17–20], and only the crystal structures of Bi₂In₄S₉ and Bi₃In₅S₁₂ were determined. In Bi₂In₄S₉, Bi atoms are unusually coordinated to five closest S forming an orthorhombic pyramid and there are both octahedrally and tetrahedrally coordinated In atoms [19], while in Bi₃In₅S₁₂ Bi atoms are eightfold (bicapped trigonal prism) and sevenfold (monocapped trigonal prism) coordinated and In atoms are octahedrally coordinated [20]. Both structures are three-dimensional framework formed by these polyhedra. Considering the small number of compounds, especially the absence of selenides and tellurides in the Bi/In/Q (Q=S, Se, Te) system, we carried out a detailed exploratory investigation in the Bi/In/Q system, which has led to the discovery of two new bismuth indium sulfides: Bi₃In₄S₁₀ and Bi_{14.7}In_{11.3}S₃₈. Interestingly, they both contain chains of Bi atoms with alternating short Bi–Bi bonds of around 3.1 Å and longer distances of around 4.6 Å. In this paper, we report the syntheses, structural characterizations, and optical properties of Bi₃In₄S₁₀ and Bi_{14.7}In_{11.3}S₃₈.

2. Experimental section

2.1. Crystal growth

The following reagents were used as obtained: Bi (Sinopharm Chemical Reagent Co., Ltd., 98+%), In (Sinopharm Chemical Reagent Co., Ltd., 99.5%), S (Sinopharm Chemical Reagent Co., Ltd., 99.5%),

and KBr (Sinopharm Chemical Reagent Co., Ltd., 99.5%). The binary starting materials, Bi_2S_3 and In_2S_3 , were synthesized by the stoichiometric reactions of elements at high temperatures in sealed silica tubes evacuated to 10^{-3} Pa. The annealing temperatures are 300°C for Bi_2S_3 and 1000°C for In_2S_3 , respectively.

Black single crystals of $\text{Bi}_3\text{In}_4\text{S}_{10}$ and $\text{Bi}_{14.7}\text{In}_{11.3}\text{S}_{38}$ were obtained via a two-step flux technique [21]. For $\text{Bi}_3\text{In}_4\text{S}_{10}$, in the first step, a mixture of In_2S_3 (0.194 g) and Bi_2S_3 (0.153 g) in a molar ratio of 2:1 was ground under Ar gas atmosphere in a drybox and loaded into a fused-silica tube. The tube was then sealed under a 10^{-3} Pa atmosphere and placed in a computer-controlled furnace. The reaction mixture was heated to 900°C in 24 h and equilibrated at this temperature for 48 h and finally cooled to room temperature by switching off the furnace. The sample thus thermally treated was used as precursor for the second-step reaction with the KBr flux (0.70 g) to grow single crystals of new phases. Upon regrinding and resealing, the precursor–flux mixture was heated to 850°C in 24 h, kept at 850°C for 96 h, then cooled at a slow rate of $4^\circ\text{C}/\text{h}$ to 300°C , and finally cooled to room temperature. The reaction product consisted of black long needles of $\text{Bi}_3\text{In}_4\text{S}_{10}$ single crystals, which were manually selected for structure characterization.

Black needles of $\text{Bi}_{14.7}\text{In}_{11.3}\text{S}_{38}$ were obtained in a similar two-step procedure. The reagents, In_2S_3 (0.097 g) and Bi_2S_3 (0.153 g) in a molar ratio of 1:1, were mixed and sealed in a fused-silica ampoule under vacuum. The reacted precursor was reground with 0.50 g KBr flux and then reheated using similar heating profiles described above.

Analyses of the crystals with an EDX-equipped Hitachi S-3500 SEM showed the presence of Bi, In, and S. The two compounds are stable in air for months.

2.2. Synthesis of pure polycrystalline materials

After the structural identification, the stoichiometric syntheses of the polycrystalline compounds were carried out using reaction mixtures as follows:



Pure polycrystalline samples of $\text{Bi}_3\text{In}_4\text{S}_{10}$ and $\text{Bi}_{14.7}\text{In}_{11.3}\text{S}_{38}$ were synthesized by solid-state reaction techniques. For the synthesis of pure $\text{Bi}_3\text{In}_4\text{S}_{10}$ powder, a mixture of In_2S_3 (1.995 g), Bi_2S_3 (2.075 g), and Bi (0.209 g) in the molar ratio of 6:4:1 was grounded and loaded into a fused-silica tube under an Ar atmosphere in a glovebox. The tube was sealed under 10^{-3} Pa atmosphere and then placed in a computer-controlled furnace. The sample was heated to 650°C in 20 h, kept at that temperature for 48 h, and then the furnace was turned off. Pure $\text{Bi}_{14.7}\text{In}_{11.3}\text{S}_{38}$ powder was prepared in a similar manner from a reaction mixture of In_2S_3 (1.105 g), Bi_2S_3 (2.165 g), and Bi (0.084 g) in the molar ratio of 339:421:40 at 600°C for 72 h.

X-ray powder diffraction of the resultant powder sample was performed at room temperature in the angular range of $2\theta = 7 - 70^\circ$ with a scan step width of 0.02° and a fixed counting time of 1 s/step using an automated Bruker D8 X-ray diffractometer equipped with a diffracted monochromator set for $\text{CuK}\alpha$ ($\lambda = 1.5418 \text{ \AA}$) radiation. The experimental powder X-ray diffraction patterns were found to be in good agreement with the calculated ones based on the single-crystal crystallographic data (Fig. 1).

2.3. Structure determination

Single-crystal X-ray diffraction data were collected with the use of graphite-monochromatized $\text{MoK}\alpha$ radiation ($\lambda = 0.71073 \text{ \AA}$)

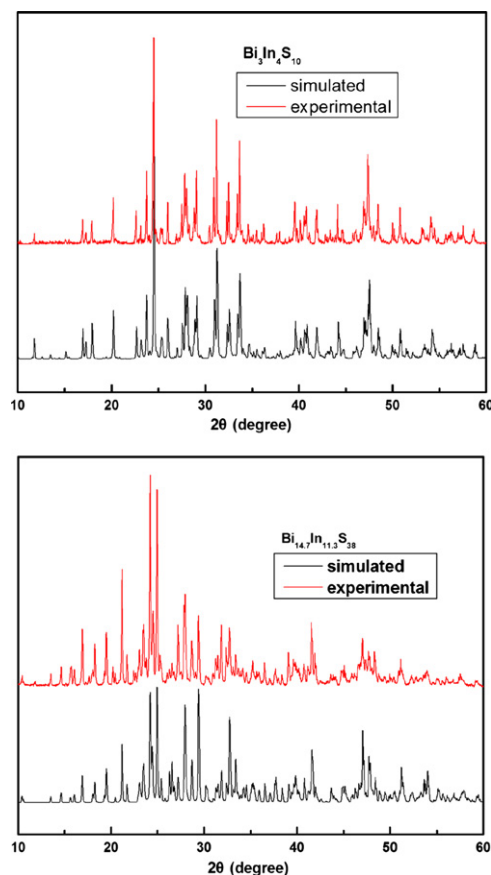


Fig. 1. Experimental (top) and simulated (bottom) X-ray powder diffraction data of $\text{Bi}_3\text{In}_4\text{S}_{10}$ (left) and $\text{Bi}_{14.7}\text{In}_{11.3}\text{S}_{38}$ (right).

at 93 K on a Rigaku AFC10 diffractometer equipped with a Saturn CCD detector. Crystal decay was monitored by re-collecting 50 initial frames at the end of data collection. The collection of the intensity data was carried out with the program Crystalclear [22]. Cell refinement and data reduction were carried out with the use of the program Crystalclear [22], and face-indexed absorption corrections were performed numerically with the use of the program XPREP [23].

The structures were solved with the direct methods program SHELXS and refined with the least-squares program SHELXL of the SHELXTL-PC suite of programs [23]. The structure of $\text{Bi}_3\text{In}_4\text{S}_{10}$ was solved in the non-centrosymmetric space group Pm . During the initial structural refinement of $\text{Bi}_3\text{In}_4\text{S}_{10}$, the site occupancies of Bi8 and Bi9 positions were allowed to refine since there were too short Bi8–Bi8' (0.615(5) Å) and Bi9–Bi9' (0.669(5) Å) contacts. The resultant occupancies of Bi8 and Bi9 were both around 0.49 and therefore they were then fixed to be 0.5 in the subsequent refinements. The flack parameter was around 0.5, which suggested a racemic twin or a centrosymmetric space group. Analysis of the atomic positions with the use of the ADDSYM in the PLATON suite of programs [24] did not reveal any additional symmetry. Thus the crystal was refined as a racemic twin with the resultant twin ratio of 0.53:0.47.

For the structure solution of $\text{Bi}_{14.7}\text{In}_{11.3}\text{S}_{38}$, seven Bi, six In, and nineteen S atoms were found by the direct methods. In the initial refinement, the isotropic displacement parameters of In1 and In4 were close to zero, which indicated partial substitution of In^{3+} by Bi^{3+} at these sites. Subsequently disorder of Bi and In was introduced at In1 and In4 positions and the refinements showed that Bi and In were disordered at the In1 and In4 positions with

Table 1
Crystal data and structure refinements for $\text{Bi}_3\text{In}_4\text{S}_{10}$ and $\text{Bi}_{14.7}\text{In}_{11.3}\text{S}_{38}$ ^a.

	$\text{Bi}_3\text{In}_4\text{S}_{10}$	$\text{Bi}_{14.7}\text{In}_{11.3}\text{S}_{38}$
fw	1406.82	5587.75
a (Å)	11.566(2)	11.386(2)
b (Å)	7.6427(15)	3.8570(8)
c (Å)	17.742(4)	34.103(7)
β (deg)	98.03(3)	94.67(3)
V (Å ³)	1553.0(5)	1492.7(5)
Space group	Pm	P2 ₁ /m
Z	4	1
ρ_c (g/cm ³)	6.017	6.216
μ (cm ⁻¹)	410.16	487.51
R(F) ^b	0.0498	0.0276
$R_w(F_o^2)^c$	0.1307	0.0646

^a For both $T=93(2)$ K and $\lambda=0.71073$ Å.

^b $R(F)=\sum||F_o|-|F_c||/\sum|F_o|$ for $F_o^2 > 2\sigma(F_o^2)$.

^c $R_w(F_o^2)=\{\sum[w(F_o^2-F_c^2)^2]/\sum wF_o^4\}^{1/2}$ for all data. $w^{-1}=\sigma^2(F_o^2)+(zP)^2$, where $P=(\text{Max}(F_o^2, 0)+2F_c^2)/3$; $z=0.07$ for $\text{Bi}_3\text{In}_4\text{S}_{10}$ and 0.03 for $\text{Bi}_{14.7}\text{In}_{11.3}\text{S}_{38}$.

Table 2
Atomic coordinates and equivalent isotropic displacement parameters (Å²) for $\text{Bi}_3\text{In}_4\text{S}_{10}$.

Atom	x	y	z	U_{eq}^a
Bi1	0.5702(2)	0.30018(14)	0.73574(15)	0.0041(2)
Bi2	0.2772(2)	0.0000	0.80397(13)	0.0083(5)
Bi3	0.5075(2)	0.24816(12)	0.98194(12)	0.0100(5)
Bi4	0.1312(2)	0.0000	0.25669(13)	0.0084(5)
Bi5	0.1304(2)	0.5000	0.25641(13)	0.0086(5)
Bi6	0.2534(2)	0.5000	0.79918(14)	0.0127(5)
Bi7	0.3718(2)	0.25061(12)	0.43606(13)	0.0137(5)
Bi8	0.0670(3)	0.0403(3)	0.50218(19)	0.0195(8)
Bi9	0.0660(3)	0.4562(3)	0.50164(19)	0.0200(8)
In1	0.9075(4)	0.5000	0.8584(3)	0.0069(9)
In2	0.7759(4)	0.0000	0.2022(3)	0.0065(10)
In3	0.6958(4)	0.5000	0.5577(3)	0.0077(9)
In4	0.2230(4)	0.5000	0.0392(3)	0.0060(9)
In5	0.4168(4)	0.2499(2)	0.1998(3)	0.0102(9)
In6	0.8988(4)	0.0000	0.8574(3)	0.0056(9)
In7	0.7362(4)	0.2490(2)	0.3802(2)	0.0058(8)
In8	0.9441(4)	0.2444(2)	0.6778(3)	0.0066(8)
In9	0.8607(4)	0.2504(2)	0.0355(3)	0.0083(9)
In10	0.2208(4)	0.0000	0.0390(3)	0.0062(9)
In11	0.6920(4)	0.0000	0.5637(3)	0.0069(9)
In12	0.7762(4)	0.5000	0.2027(3)	0.0067(10)
S1	0.4993(13)	0.0000	0.8716(8)	0.008(3)
S2	0.0364(14)	0.2483(8)	0.8149(10)	0.014(3)
S3	0.4351(15)	0.5000	0.0968(9)	0.006(3)
S4	0.4348(14)	0.0000	0.0976(9)	0.006(3)
S5	0.5000	0.5000	0.0013(8)	0.006(3)
S6	0.5990(15)	0.0000	0.4232(8)	0.006(3)
S7	0.5527(13)	0.2555(7)	0.5892(9)	0.008(3)
S8	0.6341(13)	0.2498(8)	0.2379(9)	0.011(3)
S9	0.9242(15)	0.2493(8)	0.1804(9)	0.010(3)
S10	0.7664(15)	0.2545(9)	0.8924(9)	0.013(3)
S11	0.7153(15)	0.5000	0.0572(10)	0.008(3)
S12	0.8449(14)	0.2510(15)	0.5329(9)	0.017(3)
S13	0.7993(14)	0.0000	0.7067(8)	0.007(3)
S14	0.0879(16)	0.0000	0.6495(9)	0.010(3)
S15	0.0812(16)	0.5000	0.6500(9)	0.011(3)
S16	-0.0005(16)	0.0000	-0.0001(9)	0.009(3)
S17	0.4817(14)	0.5000	0.8745(8)	0.010(3)
S18	0.1963(17)	0.2503(7)	0.1447(10)	0.016(3)
S19	0.7986(13)	0.5000	0.7059(7)	0.002(3)
S20	0.3352(13)	0.2555(7)	0.7156(7)	0.005(2)
S21	0.3057(15)	0.0000	0.5290(12)	0.025(4)
S22	0.3638(13)	0.0000	0.2912(8)	0.003(3)
S23	0.3639(13)	0.5000	0.2911(8)	0.003(3)
S24	0.3036(15)	0.5000	0.5284(12)	0.023(4)
S25	0.2750(16)	0.2463(15)	0.9472(11)	0.018(4)
S26	0.7146(15)	0.0000	0.0566(11)	0.008(3)
S27	0.8710(15)	0.5000	0.3480(9)	0.004(3)
S28	0.8698(14)	0.0000	0.3481(9)	0.004(3)
S29	0.5997(15)	0.5000	0.4194(9)	0.007(3)
S30	0.1493(12)	0.2497(8)	0.3650(8)	0.011(3)

^a U_{eq} is defined as one-third of the trace of the orthogonalized U_{ij} tensor.

Bi/In ratios of 0.235/0.765 and 0.113/0.887, respectively. The resultant R index R_1/wR_2 decreased from 0.0363/0.0930 to 0.0277/0.0646 and the largest peak/hole in difference electron density map was reduced from 13.41/−3.12 to 4.09/−2.99 e Å⁻³ with this disorder model. No detectable disorder between Bi and In was observed at other metal positions. The final stoichiometry was then refined to be $\text{Bi}_{14.7}\text{In}_{11.3}\text{S}_{38}$.

The final refinements included anisotropic displacement parameters for both compounds and a secondary extinction correction for $\text{Bi}_3\text{In}_4\text{S}_{10}$. The program STRUCTURE TIDY [25] was then employed to standardize the atomic coordinates. Additional experimental details are given in Table 1 and selected metrical data are given in Tables 2–5. Further information may be found in Supplementary material.

2.4. Diffuse reflectance spectroscopy

A Cary 1E UV–visible spectrophotometer with a diffuse reflectance accessory was used to measure the spectra of $\text{Bi}_3\text{In}_4\text{S}_{10}$ and $\text{Bi}_{14.7}\text{In}_{11.3}\text{S}_{38}$ over the range 200 nm (6.25 eV) to 2500 nm (0.50 eV).

3. Results and discussion

3.1. Syntheses

Black single crystals of $\text{Bi}_3\text{In}_4\text{S}_{10}$ and $\text{Bi}_{14.7}\text{In}_{11.3}\text{S}_{38}$ were obtained with the aid of KBr as flux. This is the first time that

Table 3
Atomic coordinates and equivalent isotropic displacement parameters (Å²) for $\text{Bi}_{14.7}\text{In}_{11.3}\text{S}_{38}$.

Atom	x	y	z	U_{eq}^a
Bi1	0.03909(4)	0.2500	0.390575(16)	0.00449(13)
Bi2	0.18695(5)	0.2500	0.500404(17)	0.01030(14)
Bi3	0.76823(4)	0.2500	0.927770(16)	0.00653(14)
Bi4	0.20853(4)	0.2500	0.761136(16)	0.00651(14)
Bi5	0.8013	0.2500	0.714713(16)	0.00455(13)
Bi6	0.58740(5)	0.2500	0.805798(18)	0.01203(15)
Bi7	0.05958(6)	0.15474(16)	0.16923(2)	0.0071(2)
In1	0.54612(7)	0.2500	0.54699(2)	0.0056(3)
Bi8	0.54612(7)	0.2500	0.54699(2)	0.0056(3)
In2	0.93103(8)	0.2500	0.04141(3)	0.0023(2)
In3	0.42596(8)	0.2500	0.95815(3)	0.0021(2)
In4	0.24912(7)	0.2500	0.63621(3)	0.0045(3)
Bi9	0.24912(7)	0.2500	0.63621(3)	0.0045(3)
In5	0.66177(8)	0.2500	0.13801(3)	0.0015(2)
In6	0.48289(8)	0.2500	0.32877(3)	0.0054(2)
S1	0.4828(3)	0.2500	0.88268(11)	0.0054(7)
S2	0.2371(3)	0.2500	0.22209(10)	0.0054(7)
S3	0.5775(3)	0.2500	0.20836(11)	0.0061(7)
S4	0.2580(3)	0.2500	0.12791(10)	0.0058(7)
S5	0.4714(3)	0.2500	0.62079(11)	0.0085(8)
S6	0.2535(3)	0.2500	0.33778(10)	0.0049(7)
S7	0.9400(3)	0.2500	0.53748(11)	0.0055(7)
S8	0.9929(3)	0.2500	0.91147(10)	0.0050(7)
S9	0.6986(3)	0.2500	0.31281(10)	0.0057(7)
S10	0.4175(3)	0.2500	0.03240(10)	0.0047(7)
S11	0.6118(3)	0.2500	0.47483(11)	0.0091(8)
S12	0.5735(3)	0.2500	0.72269(10)	0.0046(7)
S13	0.3041(3)	0.2500	0.43623(10)	0.0067(7)
S14	0.9496(3)	0.2500	0.24582(11)	0.0078(8)
S15	0.1295(3)	0.2500	0.01167(10)	0.0043(7)
S16	0.0253(3)	0.2500	0.65993(11)	0.0055(7)
S17	0.7227(3)	0.2500	0.06477(11)	0.0059(7)
S18	0.8257(3)	0.2500	0.41351(11)	0.0094(8)
S19	0.1898(3)	0.2500	0.83682(11)	0.0069(7)

^a U_{eq} is defined as one-third of the trace of the orthogonalized U_{ij} tensor.

Table 4Selected bond lengths (Å) for Bi₃In₄S₁₀.

In-1S2	2.615(13)	In9-S5	2.639(12)	Bi4-S9	3.208(14)
In1-S2	2.615(13)	In9-S9	2.573(16)	Bi4-S9	3.208(14)
In1-S5	2.619(16)	In9-S10	2.620(16)	Bi4-S18	2.932(15)
In1-S10	2.612(14)	In9-S11	2.608(12)	Bi4-S18	2.932(15)
In1-S10	2.612(14)	In9-S16	2.631(13)	Bi4-S22	2.674(15)
In1-S19	2.820(15)	In9-S26	2.615(13)	Bi4-S28	3.624(17)
In2-S8	2.650(13)	In10-S4	2.547(16)	Bi4-S30	2.695(11)
In2-S8	2.650(13)	In10-S16	2.557(19)	Bi4-S30	2.695(11)
In2-S9	2.627(14)	In10-S18	2.720(14)	Bi5-S9	3.207(14)
In2-S9	2.627(14)	In10-S18	2.720(14)	Bi5-S9	3.207(14)
In2-S26	2.581(19)	In10-S25	2.623(16)	Bi5-S18	2.928(15)
In2-S28	2.664(17)	In10-S25	2.623(16)	Bi5-S18	2.928(15)
In3-S7	2.609(12)	In11-S6	2.573(16)	Bi5-S23	2.685(15)
In3-S7	2.609(12)	In11-S7	2.611(12)	Bi5-S27	3.606(18)
In3-S12	2.647(15)	In11-S7	2.611(11)	Bi5-S30	2.701(11)
In3-S12	2.647(15)	In11-S12	2.717(15)	Bi5-S30	2.701(11)
In3-S19	2.730(14)	In11-S12	2.717(15)	Bi6-S2	3.205(15)
In3-S29	2.549(16)	In11-S13	2.665(15)	Bi6-S2	3.205(15)
In4-S3	2.522(16)	In12-S8	2.652(13)	Bi6-S15	3.082(16)
In4-S5	2.547(18)	In12-S8	2.652(13)	Bi6-S17	2.788(17)
In4-S18	2.720(14)	In12-S9	2.635(13)	Bi6-S20	2.643(11)
In4-S18	2.720(14)	In12-S9	2.635(13)	Bi6-S20	2.643(11)
In4-S25	2.657(16)	In12-S11	2.579(19)	Bi6-S25	3.245(17)
In4-S25	2.657(16)	In12-S27	2.658(16)	Bi6-S25	3.245(17)
In5-S3	2.674(12)	Bi1-S1	3.506(11)	Bi7-S6	3.285(14)
In5-S4	2.661(11)	Bi1-S7	2.601(17)	Bi7-S7	3.190(16)
In5-S8	2.510(15)	Bi1-S10	3.351(16)	Bi7-S21	2.705(14)
In5-S18	2.601(19)	Bi1-S13	3.596(12)	Bi7-S22	3.196(12)
In5-S22	2.633(11)	Bi1-S17	3.184(12)	Bi7-S23	3.193(12)
In5-S23	2.632(11)	Bi1-S19	3.159(13)	Bi7-S24	2.702(14)
In6-S2	2.653(14)	Bi1-S20	2.713(15)	Bi7-S29	3.298(14)
In6-S2	2.653(14)	Bi1-Bi1	3.054(2)	Bi7-S30	2.703(12)
In6-S10	2.604(13)	Bi2-S1	2.679(16)	Bi8-S12	3.143(17)
In6-S10	2.604(13)	Bi2-S2	3.399(15)	Bi8-S12	3.498(16)
In6-S13	2.759(15)	Bi2-S2	3.399(15)	Bi8-S14	2.610(16)
In6-S16	2.632(16)	Bi2-S14	3.260(16)	Bi8-S21	2.753(17)
In7-S6	2.658(12)	Bi2-S20	2.649(10)	Bi8-S28	3.321(16)
In7-S8	2.633(15)	Bi2-S20	2.649(10)	Bi8-S30	3.169(15)
In7-S12	2.824(16)	Bi2-S25	3.165(17)	Bi8-S30	3.520(14)
In7-S27	2.585(12)	Bi2-S25	3.165(17)	Bi8-Bi9	3.179(4)
In7-S28	2.565(12)	Bi3-S1	2.718(10)	Bi9-S12	3.114(17)
In7-S29	2.639(12)	Bi3-S3	3.005(13)	Bi9-S12	3.499(16)
In8-S2	2.516(18)	Bi3-S4	3.000(13)	Bi9-S15	2.636(16)
In8-S12	2.664(16)	Bi3-S10	3.581(19)	Bi9-S24	2.744(18)
In8-S13	2.607(11)	Bi3-S11	3.219(14)	Bi9-S27	3.303(16)
In8-S14	2.596(13)	Bi3-S17	2.697(10)	Bi9-S30	3.155(15)
In8-S15	2.605(13)	Bi3-S25	2.674(19)	Bi9-S30	3.538(13)
In8-S19	2.670(10)	Bi3-S26	3.194(14)		

crystals can be grown using the flux method in the Bi/In/Q (Q=S, Se, Te) system. In the past, crystals were only grown by the vapor transport method with the use of iodine or chlorine as the transporting agent [19,20], which might easily led to the formation of bismuth halide. According to this study, the flux method may be a valuable method for isolating new phases in the Bi/In/Q system. Furthermore, the successful syntheses of pure polycrystalline samples indicate that these two compounds are thermodynamically stable phases.

3.2. Structures

Bi₃In₄S₁₀ crystallizes in a new three-dimensional structure type (Fig. 2). Each In atom is coordinated to an octahedron of six S atoms with In–S bond lengths ranging from 2.510(15) to 2.824(16) Å, which are consistent with those of 2.508 (6)–2.833 (5) Å in Bi₃In₅S₁₂ [19]. The InS₆ octahedra are connected to each other by corner and edge-sharing to form the three-dimensional In–S sublattice (Fig. 3) with channels along the *b* direction, which are occupied by the isolated one-dimensional Bi–S sublattice

Table 5Selected bond lengths (Å) for Bi_{1.47}In_{1.3}S₃₈.

In1-S5	2.721(4)	In6-S5	2.608(3)	Bi4-S9	3.410(3)
In1-S11	2.630(4)	In6-S6	2.655(3)	Bi4-S9	3.410(3)
In1-S11	2.700(3)	In6-S9	2.559(3)	Bi4-S14	2.636(2)
In1-S11	2.700(3)	In6-S12	2.651(3)	Bi4-S14	2.636(2)
In1-S13	2.607(2)	In6-S12	2.651(3)	Bi4-S19	2.607(4)
In1-S13	2.607(2)	Bi1-S6	3.149(3)	Bi5-S2	2.951(3)
In2-S8	2.613(2)	Bi1-S7	3.114(3)	Bi5-S2	2.951(3)
In2-S8	2.613(2)	Bi1-S7	3.114(3)	Bi5-S6	2.670(3)
In2-S15	2.551(3)	Bi1-S13	3.281(4)	Bi5-S6	2.670(3)
In2-S15	2.696(3)	Bi1-S16	2.649(2)	Bi5-S12	2.629(3)
In2-S15	2.696(3)	Bi1-S16	2.649(2)	Bi5-S14	3.600(3)
In2-S17	2.563(3)	Bi1-S18	2.612(3)	Bi5-S14	3.600(3)
In3-S1	2.704(4)	Bi2-S7	2.678(2)	Bi5-S16	3.282(3)
In3-S10	2.542(4)	Bi2-S7	2.678(2)	Bi6-S1	2.967(4)
In3-S10	2.628(2)	Bi2-S7	3.176(4)	Bi6-S2	2.988(3)
In3-S10	2.628(2)	Bi2-S11	3.060(3)	Bi6-S2	2.988(3)
In3-S17	2.642(2)	Bi2-S11	3.060(3)	Bi6-S3	2.707(3)
In3-S17	2.642(2)	In6-S5	2.608(3)	Bi4-S3	3.213(3)
In4-S5	2.627(4)	Bi2-S13	2.654(4)	Bi6-S3	2.707(2)
In4-S9	2.632(3)	Bi2-S18	3.525(3)	Bi6-S4	3.359(3)
In4-S9	2.632(3)	Bi2-S18	3.525(3)	Bi6-S4	3.359(3)
In4-S16	2.736(3)	Bi3-S1	3.480(4)	Bi6-S12	2.826(4)
In4-S18	2.662(3)	Bi3-S4	2.706(3)	Bi7-Bi7	3.1222(14)
In4-S18	2.662(3)	Bi3-S4	2.706(3)	Bi7-S2	2.622(4)
In5-S1	2.596(2)	Bi3-S8	2.662(3)	Bi7-S4	2.783(3)
In5-S1	2.596(2)	Bi3-S10	3.241(3)	Bi7-S8	3.178(3)
In5-S3	2.656(4)	Bi3-S10	3.241(3)	Bi7-S8	3.597(3)
In5-S17	2.646(4)	Bi3-S15	2.991(3)	Bi7-S14	3.010(4)
In5-S19	2.660(2)	Bi3-S15	2.991(3)	Bi7-S19	3.232(3)
In5-S19	2.660(2)	Bi4-S3	3.213(3)	Bi7-S19	3.644(3)

(Fig. 4). Bi1, Bi8, and Bi9 are coordinated to a distorted bicapped trigonal prism (*btp*) of seven S and one Bi, while all other Bi atoms are coordinated in a distorted *btp* of eight S atoms. The 6s² lone pair is stereochemically active for each Bi atom with the Bi–S distances ranging from 2.601(17) to 3.624(17) Å (Table 4), which are comparable to those of 2.619(4) to 3.397(5) Å in Bi₃In₅S₁₂ [19].

Two Bi1(Bi1)(S)₇ *btps* are connected by the Bi1–Bi1 bond to form a [Bi₁2S₁₂]²⁰⁻ unit and these [Bi₁2S₁₂]²⁰⁻ units are further stacked along the *b* direction by edge-sharing. The Bi8(Bi9)(S)₇ and Bi9(Bi8)(S)₇ *btps* are connected in a similar manner via the Bi8–Bi9 bond. Such connectivity produces a row of Bi1 atoms along the *b* direction with alternating short and long distances of 3.054 (2) and 4.588(2) Å and another row of Bi8 and Bi9 atoms with alternating distances of 3.178(3) and 4.464(3) Å (Fig. 5). The short Bi...Bi distances represent Bi–Bi bonds, which are unusual in bismuth chalcogenides. Other chalcogenides possessing Bi–Bi bonds include (Bi₂Q₃)_m(Bi)_n (Q=Se, Te) [26,27,28], (BiS)_{1.1}MS₂ (M=Nb, Ta) [29,30], Bi₂M₄Q₈ (M=Al, Ga; Q=S, Se) [31], and CsBi₄Te₆ [7,9]. The arrangements of the Bi–Bi bonds in these compounds are compared in Fig. 5. In BiSe, a typical member of the (Bi₂Q₃)_m(Bi)_n (Q=Se, Te) family, each Bi is connected to three Bi atoms to form a metallic Bi layer inserted between the Bi₂Se₃ layers [27], while in CsBi₄Te₆ and (BiS)_{1.1}NbS₂ the Bi–Bi bonds are separated faraway by the (Bi₄Te₆) block [7,9] and the (BiS) block [30], respectively. As for Bi₂Ga₄S₈, although the Bi(Bi)(S)₄ square pyramid form a pair through the Bi–Bi bond, these pairs are not further connected to each other, but are separated by GaS₄ tetrahedra at a distance of 8.8876 (17) Å [31]. So even the Bi atoms may be viewed as aligned in a chain with alternating short and long distances in Bi₂Ga₄S₈, the distance between the non-bonding Bi atoms (8.8876(17) Å) is much longer than those of 4.588(2) and 4.464(3) Å in Bi₃In₄S₁₀. The Bi1–Bi1 bond length (3.054 (2) Å) and Bi8–Bi9 bond length (3.178(3) Å) in Bi₃In₄S₁₀ are comparable to those of 3.053(2), 3.238(1), 3.124(5), and 3.144(1) Å in BiSe, CsBi₄Te₆, (BiS)_{1.1}NbS₂, and Bi₂Ga₄S₈, respectively.

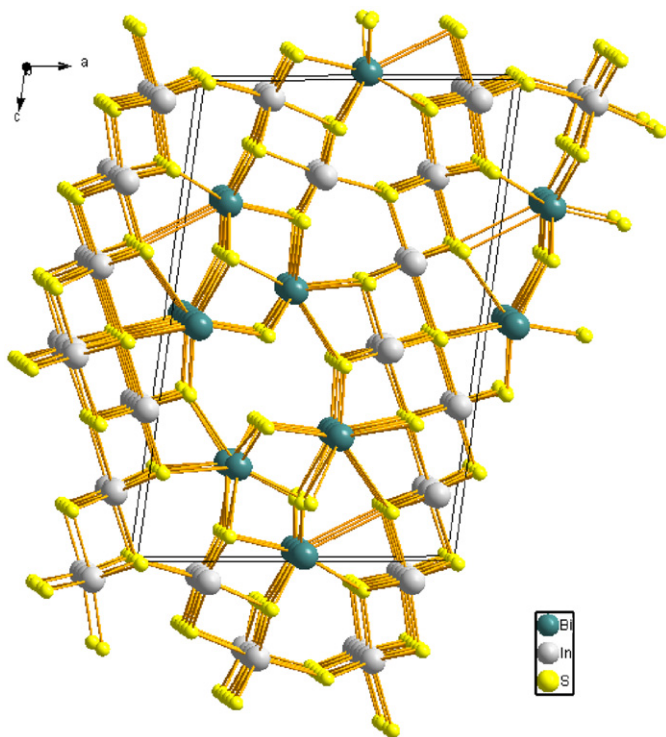


Fig. 2. Structure of $\text{Bi}_3\text{In}_4\text{S}_{10}$ viewed along [010].

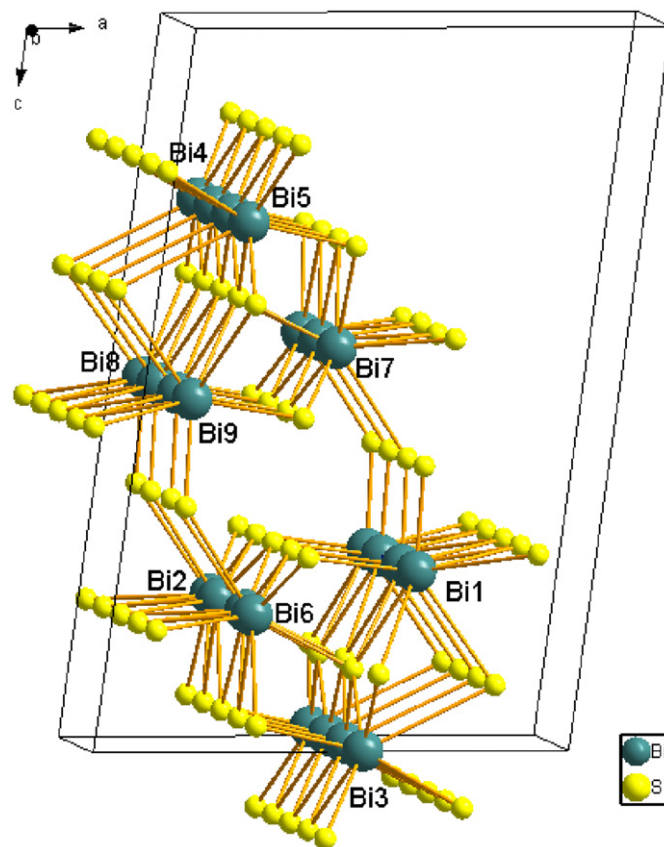


Fig. 4. Structure of the Bi–S sublattice in $\text{Bi}_3\text{In}_4\text{S}_{10}$.

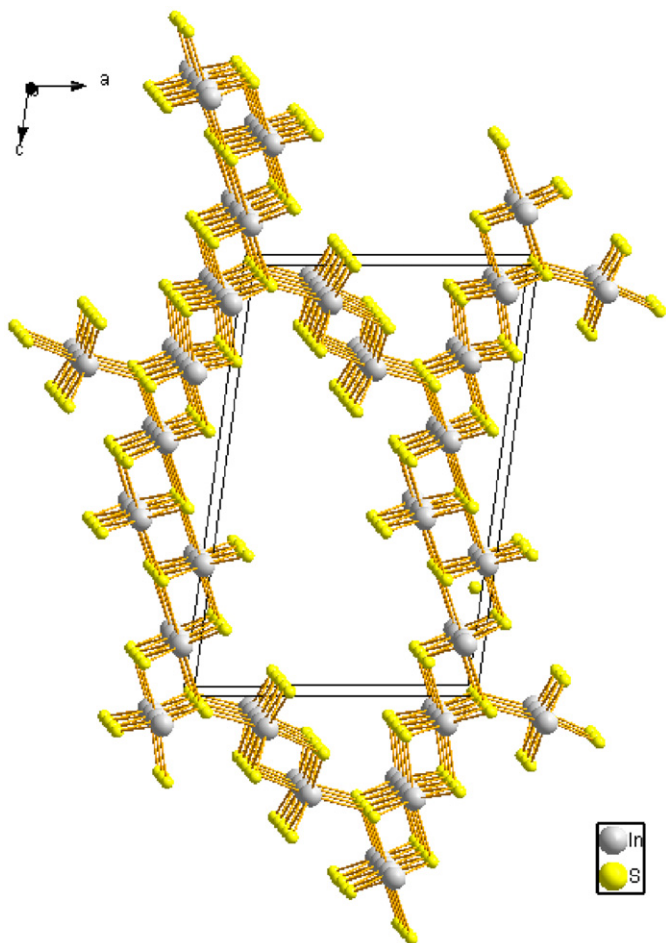


Fig. 3. Structure of the In–S sublattice in $\text{Bi}_3\text{In}_4\text{S}_{10}$.

The remaining BiS_8 *btps* form four chains along the *b* direction by face sharing. All these chains together with the $\text{Bi1 } btp \dots \text{Bi1 } btp \dots \text{Bi1 } btp \dots \text{Bi1 } btp$ chain and the $\text{Bi8 } btp \dots \text{Bi9 } btp \dots \text{Bi8 } btp \dots \text{Bi9 } btp$ chain are connected to each other by bridging S atoms and form an one-dimensional Bi–S sublattice along the *b* direction (Fig. 4). This Bi–S sublattice is then incorporated into the empty channels in the In–S sublattice to generate the three-dimensional framework (Fig. 1).

There is no S–S bond or any detectable disorder among In and Bi. From the description of the crystal structure, it is evident that Bi2 , Bi3 , Bi4 , Bi5 , Bi6 , Bi7 , and all In atoms are $3+$, while Bi1 , Bi8 , and Bi9 are $2+$. In this way the charge balance can be achieved by the formula $(\text{Bi}^{2+})(\text{Bi}^{3+})_2(\text{In}^{3+})_4(\text{S}^{2-})_{10}$.

The structure of $\text{Bi}_{14.7}\text{In}_{11.3}\text{S}_{38}$ is illustrated in Fig. 6. It is also a three-dimensional framework. In^{3+} is partially substituted by Bi^{3+} at the In1 and In4 positions. Similar substitution was observed in $\text{Pb}_4\text{In}_2\text{Bi}_4\text{S}_{13}$ [32] and $\text{Pb}_4\text{In}_3\text{Bi}_7\text{S}_{18}$ [33]. However, the amounts of Bi at the In1 and In4 positions are relatively small (23.5% and 11.3%), these two positions will be treated as the In positions in the discussion to simplify the structure description. Each In atom is coordinated to an octahedron of six S atoms with the normal In–S bond lengths of 2.551(3)–2.736(3) Å. The structure of the In–S sublattice is shown in Fig. 7. In1S_6 , In4S_6 , and In6S_6 octahedra are connected to each other by corner and edge-sharing to form a chain along the *b* direction, while In2S_6 , In3S_6 , In5S_6 octahedra are connected through corner and edge-sharing to generate a two-dimensional layer parallel to the *ab* plane.

Bi1 and Bi4 are coordinated to a distorted monocapped trigonal prism (*mtp*) of seven S atoms, and Bi2 , Bi3 , Bi4 , Bi5 , and Bi6 are coordinated to a distorted *btp* of eight S atoms, while Bi7 is

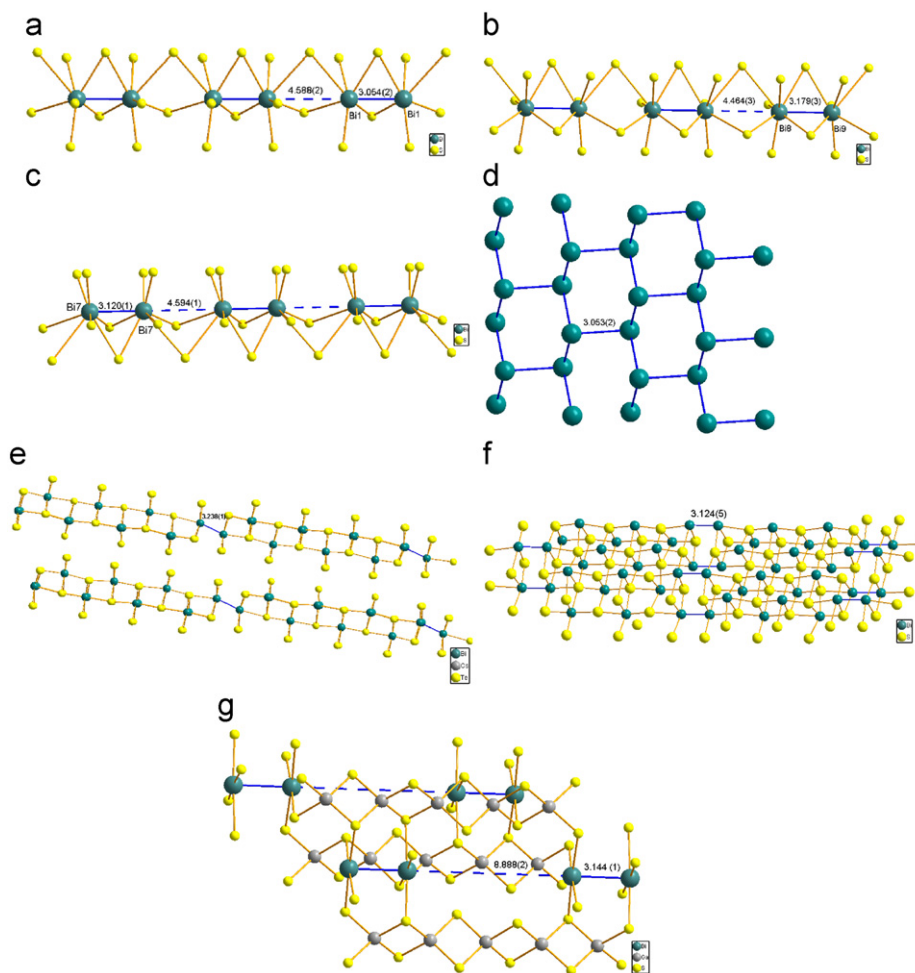


Fig. 5. Arrangements of Bi–Bi bonds in chalcogenides: (a) Bi1–Bi1 bond in $\text{Bi}_3\text{In}_4\text{S}_{10}$, (b) Bi8–Bi9 bond in $\text{Bi}_3\text{In}_4\text{S}_{10}$, (c) Bi7–Bi7 bond in $\text{Bi}_{14.7}\text{In}_{11.3}\text{S}_{38}$, (d) Bi–Bi bond in BiSe , (e) Bi–Bi bond in CsBi_4Te_6 , (f) Bi–Bi bond in $(\text{BiS})\text{NbS}_2$, and (g) Bi–Bi bonds in $\text{Bi}_2\text{Ga}_4\text{S}_8$.

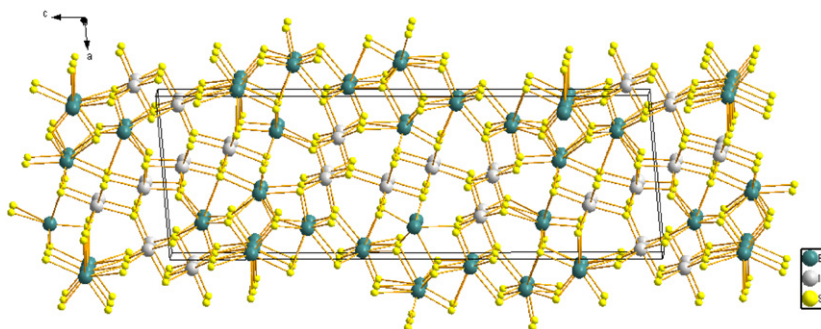


Fig. 6. Structure of $\text{Bi}_{14.7}\text{In}_{11.3}\text{S}_{38}$ viewed along [010].

coordinated to a distorted *btp* of seven S and one Bi7. The $6s^2$ lone pair also exhibits its stereochemical activity in each Bi atom with the Bi–S bond distances ranging from 2.607(4) to 3.644(3) Å (Table 5). Just as the Bi1(Bi1)(S)₇ *btps* in $\text{Bi}_3\text{In}_4\text{S}_{10}$, two Bi7(Bi7)(S)₇ *btps* in $\text{Bi}_{14.7}\text{In}_{11.3}\text{S}_{38}$ are connected by the Bi–Bi bond to form a $[\text{Bi}_7_2\text{S}_{12}^{20-}]$ unit and these $[\text{Bi}_7_2\text{S}_{12}^{20-}]$ units are further connected by two bridging S atoms (Fig. 5). In this way, the Bi7 atoms form a chain along the *b* direction with alternating short Bi7–Bi7 bonds of 3.120(1) Å and long distances of 4.594(1) Å. All the Bi–S prisms are stacked along *b*, forming chains parallel to *b*. The Bi3 *btp*, Bi4 *btp*, Bi5 *btp*, Bi6 *btp*, and Bi7 *btp* chains are connected to each

other to generate a two-dimensional layer parallel to the *ab* plane. Two such layers, related by a center of inversion, are then linked by the Bi1S₇ *mtps* and Bi2S₈ *btps* (Fig. 8). The one-dimensional void produced in this way is occupied by the chain of InS₆ octahedra, while the Bi–S layers are connected to layers of InS₆ octahedra to generate the three-dimensional framework (Fig. 6).

The disorder between Bi and In at the In1 and In4 positions has no influence on the charge balance since both Bi and In are 3+ at these two positions. There are no S–S bonds in the structure. Based on the bonding in the structure, a formula of $(\text{Bi}^{2+})_2(\text{Bi}^{3+})_{9.3}(\text{In}^{3+})_{14.7}(\text{S}^{2-})_{38}$ can be achieved with the balanced charge.

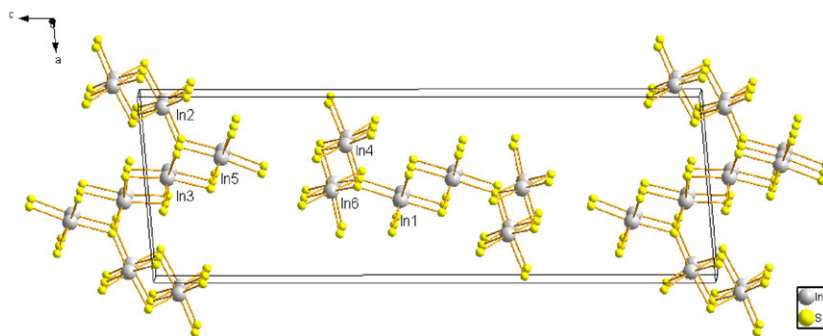


Fig. 7. Structure of the In-S sublattice in $\text{Bi}_{14.7}\text{In}_{11.3}\text{S}_{38}$.

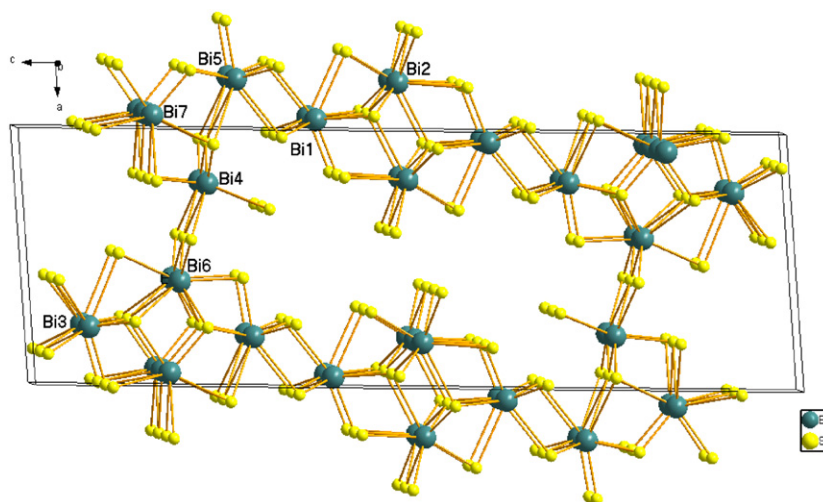


Fig. 8. Structure of the Bi-S sublattice in $\text{Bi}_{14.7}\text{In}_{11.3}\text{S}_{38}$.

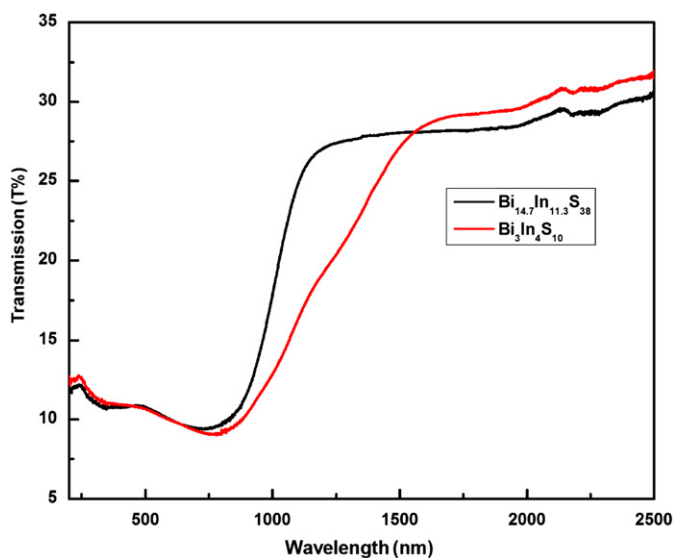


Fig. 9. Diffuse reflectance spectra of $\text{Bi}_3\text{In}_4\text{S}_{10}$ and $\text{Bi}_{14.7}\text{In}_{11.3}\text{S}_{38}$.

$\text{Bi}_3\text{In}_4\text{S}_{10}$ and 1.45(2) eV for $\text{Bi}_{14.7}\text{In}_{11.3}\text{S}_{38}$ were deduced by the straightforward extrapolation method [34].

4. Conclusion

Exploratory investigation in the Bi/In/Q system by means of a two-step flux method has led to the successful discovery of two new compounds, namely $\text{Bi}_3\text{In}_4\text{S}_{10}$ and $\text{Bi}_{14.7}\text{In}_{11.3}\text{S}_{38}$. They adopt two new types of three-dimensional framework and a characteristic feature in them is the presence of chains of Bi atoms with alternating short Bi–Bi bonds of around 3.1 Å and longer distances of around 4.6 Å. This is the first time that such chains of Bi atoms are found in chalcogenides. Based on the bonding in the structure, charge balance can be achieved by the formula $(\text{Bi}^{2+})(\text{Bi}^{3+})_2(\text{In}^{3+})_4(\text{S}^{2-})_{10}$ for $\text{Bi}_3\text{In}_4\text{S}_{10}$ and $(\text{Bi}^{2+})_2(\text{Bi}^{3+})_{9.3}(\text{In}^{3+})_{14.7}(\text{S}^{2-})_{38}$ for $\text{Bi}_{14.7}\text{In}_{11.3}\text{S}_{38}$. Our successful syntheses of the powder samples according to the above formulas further prove the correctness of the stoichiometry. From the diffuse reflectance measurements, the optical band gaps are 1.42(2) eV for $\text{Bi}_3\text{In}_4\text{S}_{10}$ and 1.45(2) eV for $\text{Bi}_{14.7}\text{In}_{11.3}\text{S}_{38}$, respectively.

Acknowledgment

This research was supported by the National Basic Research Project of China (no. 2010CB630701).

3.3. Experimental band gap

The diffuse reflectance spectra of $\text{Bi}_3\text{In}_4\text{S}_{10}$ and $\text{Bi}_{14.7}\text{In}_{11.3}\text{S}_{38}$ are shown in Fig. 9. The optical band gaps of 1.42(2) eV for

Supplemental information

The crystallographic data for $\text{Bi}_3\text{In}_4\text{S}_{10}$ and $\text{Bi}_{14.7}\text{In}_{11.3}\text{S}_{38}$ have been deposited with FIZ Karlsruhe as CSD numbers 421865 and 421866. These data may be obtained free of charge by contacting FIZ Karlsruhe at +497247808666(fax) or crysdata@fiz-karlsruhe.de (e-mail).

Appendix A. Supplementary material

Supplementary data associated with this article can be found in the online version at doi:[10.1016/j.jssc.2010.08.028](https://doi.org/10.1016/j.jssc.2010.08.028).

References

- [1] E. Makovicky, Neues Jahrb. Mineral. Abh. 160 (1989) 269.
- [2] J.D. Feichtner, G.W. Roland, Appl. Opt. 11 (1972) 993.
- [3] A.A. Ballman, R.L. Byer, D. Eimerl, R.S. Feigelson, B.J. Feldman, L.S. Goldberg, N. Menyuk, C.L. Tang, Appl. Opt. 26 (1987) 224.
- [4] I. Chung, J.-H. Song, J.I. Jang, A.J. Freeman, J.B. Ketterson, M.G. Kanatzidis, J. Am. Chem. Soc. 131 (2009) 2647.
- [5] S. Ibuki, S. Yoshimatsu, J. Phys. Soc. Jpn. 10 (1955) 549.
- [6] L.R. Testardi Jr., J.N. Bierly, F.J. Donahoe, J. Phys. Chem. Solids 23 (1962) 1209.
- [7] D.-Y. Chung, T. Hogan, P. Brazis, M. Rocci-Lane, C. Kannewurf, M. Bastea, C. Uher, M.G. Kanatzidis, Science 287 (2000) 1024.
- [8] M.G. Kanatzidis, T.J. McCarthy, T.A. Tanzer, L.-H. Chen, L. Iordanidis, T. Hogan, C.R. Kannewurf, C. Uher, B. Chen, Chem. Mater. 8 (1996) 1465.
- [9] D.-Y. Chung, T.P. Hogan, R.-L. Melissa, P. Brazis, J.R. Ireland, C.R. Kannewurf, M. Bastea, C. Uher, M.G. Kanatzidis, J. Am. Chem. Soc. 126 (2004) 6414.
- [10] D.-Y. Chung, K.-S. Choi, L. Iordanidis, J.L. Schindler, P.W. Brazis, C.R. Kannewurf, B. Chen, S. Hu, C. Uher, M.G. Kanatzidis, Chem. Mater. 9 (1997) 3060.
- [11] J. Yao, B. Deng, D.E. Ellis, J.A. Ibers, Inorg. Chem. 41 (2002) 7094.
- [12] F.Q. Huang, R.C. Somers, A.D. McFarland, R.P. Van Duyne, J.A. Ibers, J. Solid State Chem. 174 (2003) 334.
- [13] F.Q. Huang, K. Mitchell, J.A. Ibers, J. Alloys Compd. 325 (2001) 84.
- [14] A. Mrotzek, M.G. Kanatzidis, Acc. Chem. Res. 36 (2003) 111, 36.
- [15] V. Petrov, A. Yelisseyev, L. Isaenko, S. Lobanov, A. Titov, J.-J. Zondy, Appl. Phys. B: Lasers Opt. 78 (2004) 543.
- [16] R. Klenk, J. Klaer, R. Scheer, M.Ch. Lux-Steiner, I. Luck, N. Meyer, U. Ruehle, Thin Solid Films (2005) 480.
- [17] V. Krämer, Thermochim. Acta 86 (1985) 291.
- [18] V. Krämer, Thermochim. Acta 15 (1976) 205.
- [19] V. Krämer, Acta Crystallogr. B36 (1980) 1922.
- [20] G. Chapuis, C.H. Gnehm, V. Krämer, Acta Crystallogr. B28 (1972) 3128.
- [21] H.-Y. Zeng, H. Mattausch, A. Simon, F.-K. Zheng, Z.-C. Dong, G.-C. Guo, J.-S. Huang, Inorg. Chem. 45 (2006) 7943.
- [22] CrystalClear, Rigaku Corporation, Tokyo, Japan, 2008.
- [23] G.M. Sheldrick, Acta Crystallogr. A 64 (2008) 112.
- [24] A.L. Spek, J. Appl. Crystallogr. 36 (2003) 7.
- [25] L.M. Gelato, E. Parthé, J. Appl. Crystallogr. 20 (1987) 139.
- [26] H. Lind, S. Lidin, Solid State Sci. 5 (2003) 47.
- [27] K. Yamana, K. Kihara, T. Matsumoto, Acta Crystallogr. B 35 (1979) 147.
- [28] Y. Feutelais, B. Legendre, N. Rodier, V. Agafonov, Mater. Res. Bull. 28 (1993) 591.
- [29] Y. Gotoh, M. Onoda, J. Akimoto, M. Goto, Y. Oosawa, Jpn. J. Appl. Phys. 31 (1) (1992) 3946.
- [30] Y. Gotoh, J. Akimoto, M. Goto, Y. Oosawa, M. Onoda, J. Solid State Chem. 116 (1995) 61.
- [31] H. Kalpen, W. Hoënle, M. Somer, U. Schwarz, K. Peters, H.G. von Schnering, Z. Anorg. Allg. Chem. 624 (1998) 1137.
- [32] V. Krämer, Acta Crystallogr. C42 (1986) 1089.
- [33] V. Krämer, I. Reis, Acta Crystallogr. C42 (1986) 24.
- [34] O. Schevciw, W.B. White, Mater. Res. Bull. 18 (1983) 1059.